Investigation of Low-Lying States of Oxygen Molecule via Second-Order Multireference Perturbation Theory: A State-Specific Approach

Sudip Chattopadhyay,*,† Uttam Sinha Mahapatra,‡,⊥ and Rajat K. Chaudhuri§,#

Department of Chemistry, Bengal Engineering and Science University, Shibpur, Howrah 711 103, India, Department of Physics, Taki Government College, Taki, North 24 Parganas, India, and Indian Institute of Astrophysics, Bangalore 560034, India

Received: December 11, 2008; Revised Manuscript Received: March 24, 2009

The relative performance of four variants of the Møller−Plesset (MP) partitioning (using different diagonal one-electron unperturbed Hamiltonian, H_0) based state-specific multireference perturbation theory (SS-MRPT) [termed as SS-MRPT(MP)] has been investigated and demonstrated by calculations of the dissociation potential energy curves (PECs) of the first three electronic states [ground state $X^3\Sigma_g^-$ as well as low-lying singlet excited states, $a^1\Delta_g$ and $b^1\Sigma_g^+$] of the oxygen molecule using different basis sets. The spectroscopic constants extracted from the computed PECs obtained by the SS-MRPT(MP) method are calibrated with respect to the corresponding value of the full configuration interaction (FCI) and experimental data for the corresponding states. We have also computed vertical excitation (or transition) energies and compared those with the corresponding FCI values along with the results of other available sophisticated methods. Encouraging agreement between SS-MRPT(MP) theory and some benchmark calculations has been observed. We have thus assessed the applicability and accuracy of the SS-MRPT(MP) method with different diagonal one-electron partitioning schemes. The ability of the SS-MRPT(MP) method with different partitioning schemes to predict full PECs and spectroscopic constants of the ground state and excited states with almost equivalent accuracy is promising.

I. Introduction

It is now well documented in the literature that the Møller−Plesset (MP) perturbation (MP) theory is a very effective and popular ab initio approach that has been used over the last few decades to compute dynamic electron correlation. Although the single-reference (SR) MP perturbation theory (SR-MPPT)[1,2] is well known as an efficient many-body approach to treat electron correlation in an efficient and size-extensive way in the absence of quasidegeneracy where static correlation prevails, several studies have seriously questioned the use of low-order/higher-order SR-MPPT to describe electron correlation effects when quasidegenerate boundary orbitals are encountered (this happens, for example, during bond breaking, for highly distorted geometries, for diradicals, and so forth) in atomic and molecular calculations.[2,3] The problem of SR-based methods in the presence of quasidegenerate electronic configurations has stimulated several new developments in the realm of electronic structure theory. The presence of quasidegeneracy is also frequently observed if one wants to compute the dissociation potential energy curves (PECs) over the entire range of geometries (including the bond-breaking region). The generation of precise and reliable PECs of spectroscopic accuracy is perhaps one of the most difficult problems faced by electronic structure theory.[4] Since during a reaction bonds are broken and re-formed, a single-determinant description is not of consistent quality. As the multireference(MR) techniques can easily handle quasidegeneracy (nondynamical correlation), the multiconfigurational SCF (MCSCF) approach [usually the complete-active-space self-consistent field (CASSCF) is the popular one, in which one defines an active space of orbitals and corresponding electrons that are appropriate for a chemical process of interest] remedies these shortcomings by including all configurations that are important in various regions of the potential energy, creating a qualitatively correct zeroth-order wave function. However, CASSCF cannot provide chemically accurate energetics and remains an exponential bottleneck behind dynamically corrected treatments built upon it. Though the use of a MR function is a useful prerequisite for obtaining a consistent description and it ensures a proper description of the nondynamical correlation energy, it is not sufficient since, in general, the dynamical correlation energy, which is essentially impossible to include to a significant extent in MCSCF/CASSCF, changes with the molecular geometry. Hence, for an accurate determination of the dissociation PECs of molecular systems, the inclusion of nondynamical and dynamical correlations is indispensable. Hence, in order to handle the quasidegeneracy of the reference state (usually appears when stretching and/or breaking bonds, transition states, radicals, and so forth), one has to resort to a MR-type formalism. The past few decades have seen an extraordinary growth in novel new MR-based methods and creative implementations of these methods. With current methodology, MR configuration interaction (MRCI)[5] is the only method in common use for determining spectroscopic-quality PECs. As the size of the system increases, the quality of the MRCI wave function degrades, leading to a need for size-consistent (or at least approximately size-consistent) methods, including multireference perturbation theory (MRPT) or multireference coupled-cluster (MRCC) methods.[6,7]

* To whom correspondence should be addressed. E-mail: sudip_chattopadhyay@rediffmail.com.
† Bengal Engineering and Science University.
‡ Taki Government College.
§ Indian Institute of Astrophysics.
⊥ E-mail: uttam.mahapatra@linuxmail.org.
E-mail: rkchaudh@iiap.res.in.

10.1021/jp810910n CCC: $40.75
Published on Web 04/28/2009

Over the years, the MR perturbation theory (MRPT) has proved to be a useful and versatile ab initio (nonempirical) method for accurate calculations of electron correlation of small to large size atomic and molecular systems over the entire range of PECs at a reasonably low cost in computer time. From the literature, it is evident that there has been a lot of work in the methodological development and applications of MRPT over the last few decades.[8−27] In the MRPT approach, the multiconfigurational (MC) reference function is corrected toward the exact one using the perturbation approach. The MRPT based on MC reference functions has become a basic and practical tool for studying the electronic structures of molecules and the PECs of chemical reactions. Several versions of MRPT are now included in various program packages such as GAMESS and MOLCAS. MRPT takes account of both static and dynamic electron correlations, and thus, one can obtain accurate relative energies, including reaction, activation, and excitation energies, within chemical accuracy (i.e., a few kcal/mol). At this point, we want to mention that the effective Hamiltonian-based MRPT method where the reference space contains all configurations needed for a proper zeroth-order description does not give uniform accuracy over much of the PEC due to very small or vanishing energy denominators caused by the effect of intruder states[28−30] (can lead to singularities at certain points on the PEC), which significantly limits its applicability. The intruder state problem originates when an excited electronic state outside of the model space drops into the energy regime of the chosen zeroth-order manifold in some region of the PEC. The main difficulty in excited-state PEC calculations is the intruder state problem. Though much less likely, this may also occur in ground-state PEC calculations. For this very reason, recently, this problem has been demonstrated in several investigations on MC perturbation theory, both theoretically and numerically, and remedies for improving convergence in MR theories have been given. Very hopeful developments have been recently reported in this direction. The recent focus of the MRPT development is on the state-specific (SS) approaches, which are free from intruder effects by construction, and this has led to the development of a plethora of MRPT approaches that belong to this designation. Actually, SS theories aim at treating one state at a time through a wave operator that lifts only one state, and thereby, SS theories achieve two major improvements with respect to the traditional effective Hamiltonian-based MRPT; (i) they avoid the intruder state problem and (ii) maximize accuracy for the state of interest. The formulation of complete model space (CMS)- or complete active space (CAS)-based spin-free state-specific second-order multireference perturbation theory (SS-MRPT) proposed by Mukherjee and co-workers[26,27] a few years ago is now recognized as a reliable and efficient single root or state-specific MRPT approach for the study of real chemical problems with MR character in an intruder-free manner. The key idea underlying the SS-MRPT is that once the state-specific nondynamical correlation is adopted through MR functions, what remains is mainly the dynamical correlation, which is computed by the second-order perturbation theory based on the MR function for a relatively low computational cost. The SS-MRPT is devoid of the intruder state problem in a size-extensive manner. From the very mode of the derivation of the cluster finding equation(s), it is evident that the SS-MRPT scheme is numerically more stable as long as the state energy is energetically well separated from the virtual functions. The SS-MRPT method can be used, for example, to predict bond dissociation with reasonable accuracy. This method can be considered as an attractive MRPT approach for the determination of accurate PECs as it (i) is a genuine MR method that treats all references in the model space on an equal footing and hence is effective in the context of multireferencial quantum chemical situations, (ii) leads to size-consistent energies when localized orbitals are used, and (iii) is computationally cost-effective. Very recently, several applications of the SS-MRPT with MP partitioning to molecular electronic states with different spin states have been presented and discussed by Mahapatra et al.[31] The previous applications revealed the SS-MRPT method to be a rather accurate viable tool for studying quasidegeneracy of varying degrees across the PEC in a size-extensive and spin-free manner while bypassing intruders. Of course, caution is warranted in extrapolating this conclusion to more realistic chemical systems of arbitrary size. Further calculations will be necessary to investigate how the method performs for the electronically excited states and larger molecules. A difficulty in excited-state calculations is that the states are not always well separated from the other states (intruder state problem). This may also occur, though much less likely, in ground-state calculations. More definitive conclusions can be made after the development of the SS-MRPT code capable of treating larger molecules of arbitrary complexity with extensive basis sets. Despite the success of the SS-MRPT method, there is still scope for further improvements.

Our aim in this paper is to assess the stability of the explicitly spin-free SS-MRPT(MP) method of Mukherjee and co-workers[27] for the dissociation potential curve of valence states of an oxygen molecule using a different diagonal one-electron H_0, termed H_0(OE). The oxygen molecule is thermodynamically reactive yet kinetically nonreactive. The reason for this unusual behavior is the triplet ground state of the molecule, which prevents reactions with singlet-state molecules to proceed as they are "spin forbidden" and occur only slowly at room temperature. Many processes in biology utilizing the thermodynamic reactivity of oxygen have evolved. Thus, a theoretical study of low-lying PECs (including the ground state) of an oxygen molecule helps a lot to understand these phenomena. Here, we have applied the SS-MRPT(MP) method to compute the ground [$X^3\Sigma_g^-$ ($1\sigma_g^2 1\sigma_u^2 2\sigma_g^2 2\sigma_u^2 1\pi_u^4 3\sigma_g^2 1\pi_g^1 1\pi_g^1$)] as well as low-lying excited states [say, $a^1\Delta_g$ ($1\sigma_g^2 1\sigma_u^2 2\sigma_g^2 2\sigma_u^2 1\pi_u^4 3\sigma_g^2 1\pi_g^2$) and $b^1\Sigma_g^+$ ($1\sigma_g^2 1\sigma_u^2 2\sigma_g^2 2\sigma_u^2 1\pi_u^4 3\sigma_g^2 1\pi_g^1 1\pi_g^1$)] of the oxygen molecule (which have electron-dense multiple bonds; examples of double-bond dissociation) to illustrate its performance. The ground state, $X^3\Sigma_g^-$, has two unpaired electrons with like spins in the $\pi 2p_x$ and $\pi 2p_y$ orbitals. Rearrangement of the electron spins within these two degenerate orbitals results in two possible singlet excited states. The first excited state ($a^1\Delta_g$) has two paired electrons that occupy the same molecular orbital (note there are two molecular orbitals that these electrons can occupy). The second excited state ($b^1\Sigma_g^+$) is also a singlet state with two unpaired and antiparallel electron spins. The $a^1\Delta_g$ state (with an A_g component) has the same symmetry as the $b^1\Sigma_g^+$ state in the D_{2h} computational subgroup used in the computations. In both forms of singlet O_2, the spin restriction is removed so that the oxidizing ability is greatly increased with respect to the triplet one. The molecule in both forms of the "singlet" states is particularly reactive, and the species in the first excited state is a molecule of concern in biology (singlet oxygen can react with many kinds of biological molecules such as DNA, proteins, and lipids). Therefore, a better understanding of its chemical and physical nature are important. The above-mentioned three states remain qualitatively similar to their form at the equilibrium ground-state geometry. A proper understanding and description of these states is still a challenging problem for theoreticians

as the systems show varying degrees of quasidegeneracy and would be plagued by intruders with the change of geometries[32] and hence are appropriate to test the efficacy of the different SS methods such as SS-MRPT(MP). A great variety of methods have been used for theoretical investigations of the low-lying excited states as well as the ground state.[32−34] To judge the accuracy and stability of the computed PECs, we have presented a comparison with other available many-body methods along with the corresponding FCI values (whenever available). We have reported the various spectroscopic parameters (such as r_e and ω_e) as well as the energetics of the bond-breaking process (dissociation energy D_e). We have also applied the SS-MRPT(MP) method to compute the excitation/transition energies. The spectroscopic constants have been obtained from polynomial fits to the computed PECs. Variations of the degree or the number of points had virtually no effect on the computed spectroscopic constants. The dissociation energies have been computed as the difference of the energy at a very large distance and the fitted energy minimum. In our applications, the GAMESS(US) package has been used to compute all of the one-electron and two-electron integrals (as well as one- and two-body density) in the molecular orbital (MO) basis. We might infer from our calculations that the SS-MRPT(MP) method may be considered as a useful tool to compute the PECs of the ground as well as excited states as long as the target state energy is well separated from the energies of the virtual functions.

At this point, we want to mention the fact that to get accurate results of the state energy and spectroscopic constants, one has to be sure that one (i) has reached the basis set limit; (ii) is at a sufficiently high level of the treatment of electron correlation; and (iii) has taken care of relativistic, adiabatic, and non-adiabatic corrections. Hence, more studies are needed to analyze the effect of the size of basis set and relativistic correction on the SS-MRPT(MP) results.

In the remainder of this paper, we outline the working equations of the SS-MRPT approach and then present results for the first three electronic states of the oxygen molecule. The summary of our conclusions is presented in the final section.

II. Method Section

In this section, a brief summary is provided for the SS-MRPT approach as the formal development of the SS-MRPT and its spin-free version have been described in length in several articles.[26,27] Here, we present the main issues and working equations of the spin-free SS-MRPT method. This method can be considered as a consistent generalization of the famous Møller−Plesset many-body perturbation theory for multidimensional model spaces within the state-specific framework.

In the SS-MRPT method, (a CAS-based state-specific Hilbert-space MRPT approach), each model function is treated on the same footing, and a reference function can be written as follows

$$\psi_0^{\alpha} = \sum_{\mu} c_{\mu}^{\alpha} \phi_{\mu} \tag{1}$$

where the index α represents the specific state to be studied (hence the name state-specific).

The SS-MRPT treats one state at a time by building a state-specific wave operator (relies on the Jeziorski−Monkhorst wave operator ansatz)[6] and selecting one root of an effective Hamiltonian. The Jeziorski−Monkhorst wave operator ansatz based SS scheme introduces the problem of sufficiency conditions because the number of equations that can be derived by introducing a state-specific wave operator into the Schrödinger equation is less than the number of t amplitudes contained in the cluster T^{μ} operators.[26] In the SS-MRPT, the functional dependences of the cluster amplitudes of T^{μ} and T^{ν} inducing the transition on the active spin orbitals are the same. Due to the intermediate normalization (which implies the nonhermit nature of the effective Hamiltonian), the cluster amplitudes corresponding to the internal excitations are set to 0 as CAS is assumed. The cluster amplitudes, t_{μ}^{l}, finding equation (for a given α state) can be expressed as

$$t_{\mu}^{l(1)} = \frac{H_{l\mu} + \sum_{\nu}^{\nu \neq \mu} \langle \chi_1^{\mu} | T^{\nu(1)} | \phi_{\mu} \rangle H_{\mu\nu} (c_{\nu}/c_{\mu})}{[(E_0 - H_{\mu\mu}) + (H_{\mu\mu}^0 - H_{ll}^0)]} \tag{2}$$

and the coefficients and the energy of the target state are generated by diagonalizing an effective operator (non-Hermitian) $\tilde{H}_{\mu\nu}^{(2)}$ defined in CMS (or CAS)

$$\sum_{\nu} \tilde{H}_{\mu\nu}^{(2)} c_{\nu}^{(2)} = E^{(2)} c_{\mu}^{(2)} \tag{3}$$

Since the theory is state-specific, only one eigenvalue represents the exact energy, while the remaining eigenvalues have no physical meaning. Here, $H_{\mu} = \langle \chi_l | H | \phi_{\mu} \rangle$, $H_{\mu\nu} = \langle \phi_{\mu} | H | \phi_{\nu} \rangle$, $H_{\mu\mu}^0 = \langle \phi_{\mu} | H_0 | \phi_{\mu} \rangle$, $H_{ll}^0 = \langle \chi_l | H_0 | \chi_l \rangle$, and $\tilde{H}_{\mu\nu}^{(2)} = H_{\mu\nu} + \sum_l H_{\mu l} t_{\nu}^{l(1)}$. The χ_l^{μ} stands for a general mono/biexcitation from the ϕ_{μ}. H_0 is the zeroth-order Hamiltonian. The robustness of the energy denominators in the presence of the intruder is manifested in eq 2. The denominator does not suffer convergence difficulties or singularities (intruder effects) as long as the target-state energy is well separated from the energies of the virtual functions. This situation is usually observed for the ground state.

In the SS-MRPT(MP) scheme, we have used a multipartition strategy in that the unperturbed H_0 is chosen to be dependent on the model space function ϕ_{μ} that it acts upon so that the H_0 for the function ϕ_{μ} is a sum of the diagonal parts of the Fock-like operator, f_{μ}, with respect to ϕ_{μ}. In the SS-MRPT approach, the cluster finding equation, eq 2, explicitly contains the eigenvector coefficients c_{μ}, in contrast to the state-universal MRPT approach (a multiroot scheme suitable for mapping a manifold of PECs and plagued by intruder state problems). In this formalism, the same χ_1^{μ} can also be reached by the action of specific components of operator T^{ν} on ϕ_{μ}; the corresponding cluster amplitudes are t_{ν}^{l} (that is, $\langle \chi_1^{\mu} | T^{\nu} | \phi_{\mu} \rangle$), and in this way, T^{ν} and T^{μ} are coupled. The above equation, eq 2 is a coupled equation involving the cluster amplitudes and model space coefficients. The coupling term takes care of both the redundancy and size-extensivity of the formalism refereed to the same vacuum [both the bra and ket refer to the same reference μ (CSF)] and thus is not difficult to implement. The solution of eq 2 requires the storage of only those t_{μ} amplitudes for various μ's which are labeled by the same orbital indices.

In this paper, several reasonable propositions differing in the particular choice of the one-electron zeroth-order Hamiltonian H_0 have been considered. The one-particle operators in H_0 in the MP partition are essentially various forms of diagonal elements of some Fock-like operator, defined for every model function. This corresponds to a multipartitioning strategy,[29] where unperturbed orbital energies depend on the model function. A special choice is, of course, the widely used state-averaged variant of the Fock operator, which has also been considered. It seems, however, that all of them are capable of combining the strict size consistency with high reliability of lowest-order results and rapid convergence. We now discuss the different strategies of the definition of diagonal H_0(OE) adopted by us in this work.

The simplest choice of the Fock operator is the following (called [I] in this article), and the corresponding SS-MRPT(MP) method is written as SS-MRPT(MP)[I]

$$f_\mu = \sum_{ij}\left[f^{ij}_{\text{core}} + \sum_u \left(V^{ju}_{iu} - \frac{1}{2}V^{uj}_{iu}\right)D^{\mu}_{uu}\right]\{E^j_i\} \tag{4}$$

where u represents both a doubly occupied and a singly occupied active orbital in ϕ_μ and the D^{μ}'s are the densities labeled by the active orbitals. Since our H_0 is always diagonal for the MP scheme, the zeroth-order Hamiltonian is $H^{\mu}_0 = \sum_i f_\mu{}^{ii}\{E^i_i\}$.

In this article, we also consider another physically appealing Fock operator (termed SS-MRPT(MP)[II]), which is defined with respect to $\phi_{0\mu}$ (the highest closed-shell component of a model function ϕ_μ), and it not only includes the Fock potential of the doubly occupied active orbitals included in $\phi_{0\mu}$ but also, via the blocks involving the direct spectator scattering of the singly occupied active orbitals, takes care of interaction of electrons in them. This is given by

$$\tilde{f}_\mu = \sum_{ij}[f^{ij}_{0\mu} + \sum_{u_s} V^{ju_s}_{iu_s}]\{E^j_i\} \tag{5}$$

where the normal ordering is with respect to $\phi_{0\mu}$ and where u_s represents a singly occupied active orbital in ϕ_μ. The $f_{0\mu}$ is the Fock operator for $\phi_{0\mu}$. With this choice for the Fock operator, the zeroth-order Hamiltonian for MP partitioning is $H^{\mu}_0 = \sum_i \tilde{f}_\mu{}^{ii}\{E^i_i\}$.

In addition to the above type of Fock operators, f_μ and $\tilde{f}_\mu$, we also consider their generalized forms $f = \sum_\mu f_\mu c^2_\mu$ (termed SS-MRPT(MP)[III] in this article) and $\tilde{f} = \sum_\mu \tilde{f}_\mu c^2_\mu$ (called SS-MRPT(MP)[IV]), respectively. Then, the corresponding zeroth-order Hamiltonian is expressed as $H^{\mu}_0 = \sum_i f^{ii}\{E^i_i\}$ and $H^{\mu}_0 = \sum_i \tilde{f}^{ii}\{E^i_i\}$, respectively.

In our previous works,[27,31] it has been observed that the SS-MRPT method appears to be promising and cost-effective for many applications. In the next section, we present applications of the spin-free multipartitioning SS-MRPT (restricted to second order) to the calculations of three lowest electronic states and energy splitting between molecular electronic states with different spin multiplicities of an oxygen molecule.

III. Application

This section is devoted to the discussion of the results obtained with the various variants of the SS-MRPT(MP) methods. Our particular interest here is to see whether the SS-MRPT can avoid intruders and also to discern which partitions work better and can capture a major portion of the dynamical correlation energy despite the approximations made on the excitations. In the next part, we have demonstrated that there are no significant deviations as compared to the FCI results (whenever available) in the general trend of the results for any of the chosen Fock operators in MP partitioning.

For the demonstration and assessment of the accuracy and potential of the SS-MRPT(MP) method, a study of some low-lying states including the ground state of the oxygen molecule has been carried out. These states of the molecule have been studied by several workers previously to judge the applicability of various SR- and MR-based methods. For this reason, we have decided to revisit this system with the SS-MRPT(MP) method. To check the effectiveness of the SS-MRPT(MP) with a different description of diagonal H_0(OE) in recovering the correlation energy with regard to FCI and standard many-body methods, we have carried out numerical investigations to compute the state energies over a wide range of geometries (i.e., PEC) and the spectroscopic constants of the ground state $X^3\Sigma^-_g$ as well as low-lying excited states $a^1\Delta_g$ and $b^1\Sigma^+_g$ of the oxygen molecule. Spectroscopic constants are as important as the energies themselves. Because of the complicated electronic and geometric structure of some of its electronic states, oxygen has been the subject of a large number of theoretical investigations.[32] The two excited states have a pronounced multireference character, and the degree of degeneracy can be varied continuously due to the variation of bond length; hence, this system is a very good benchmark test case to assess the performance and accuracy of the SS-MRPT(MP) method. We have used the same atomic basic sets (DZP), and scheme(s) as that of Bauschicher and Langhoff.[33] We use the D_{2h} point group and an eight electron six active orbitals [$3a_g1b_{3u}1b_{2u}1b_{2g}1b_{3g}3b_{1u}$] (8e,6v) CAS function. Although the present DZP basis set is not large enough, it is adequate to enable one to draw useful conclusions regarding the applicability of the SS-MRPT method in computing various spectroscopic constants. We have also computed various spectroscopic constants including the vertical excitation energy using Dunning's correlation consistent basis sets, cc-pVTZ and cc-pVQZ.[37] In these calculations, the 1s orbital of oxygen has been excluded from the correlation treatment. In the case of the DZP basis,[34] the reliability of the different SS-MRPT(MP) variants is assessed by comparison to the FCI results. We have performed frozen core FCI calculation at some geometries for all of the states considered here. In the case of the cc-pVTZ and cc-pVQZ basis sets, we have compared the SS-MRPT(MP) results with the well-tested multireference methods which are specifically designed to describe bond-breaking reactions due to inaccessibility of FCI calculations. For the sake of comparison of the performance of the SS-MRPT(MP) method with the MRMPPT method of Hirao and co-workers,[17] we have also calculated the dissociation PECs of the $X^3\Sigma^-_g$ and excited state $a^1\Delta_g$ of the oxygen molecule using the DZP basis via the MRMPPT method (available in GAMESS). The calculations of the singlet states reported in the present work have all been performed using state-averaged (SA) canonical CASSCF orbitals obtained by varying orbitals to minimize the weighted sum of the CASSCF energies (carried the same weight). There is no difficulty in obtaining the CASSCF wave function for the $X^3\Sigma^-_g$.

It is pertinent to highlight that both the excitation as well as the vertical excitation energies have been calculated by us. While the former has been calculated for each of the involved states with their respective equilibrium geometries, the latter calculation, on the contrary, retains the traditional description of the vertical excitation energy and has been calculated with the equilibrium bond distance corresponding to the ground state.

In Figures 1−3, we have plotted the total energy of the $^3\Sigma^-_g$, $a^1\Delta_g$, and $b^1\Sigma^+_g$ states of O_2 along with FCI for the DZP basis using different definitions of diagonal H_0(OE) considered in this paper. The correct shape of the PECs is retrieved by applying the computationally inexpensive SS-MPRT(MP) approaches. The PECs generated using different SS-MRPT(MP) schemes are obtained as a smooth and continuous curve close to the corresponding FCI results throughout the single and multireference regions of geometric configuration space for all of the different bond lengths. From these figures, it is clear that all of the SS-MRPT(MP) schemes considered here provide qualitatively correct PECs. From Figure 1, we have observed that the PECs generated via SS-MRPT(MP) schemes are very close to one another. In our calculations, we have noticed that the PECs generated via CASSCF are significantly higher in energy than the exact FCI curve (see Tables 1, 3, and 4), but they have the correct shape (see Figure 4). We also want to mention that the deviation of the CASSCF results from the FCI in the region of

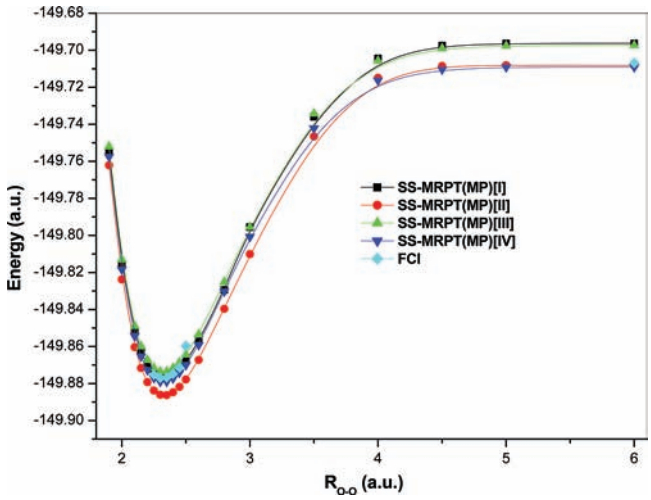

Figure 1. Plot of the dissociation potential energy curves of the ground electronic state ($^3\Sigma_g^-$) of the O_2 molecule using the DZP basis.

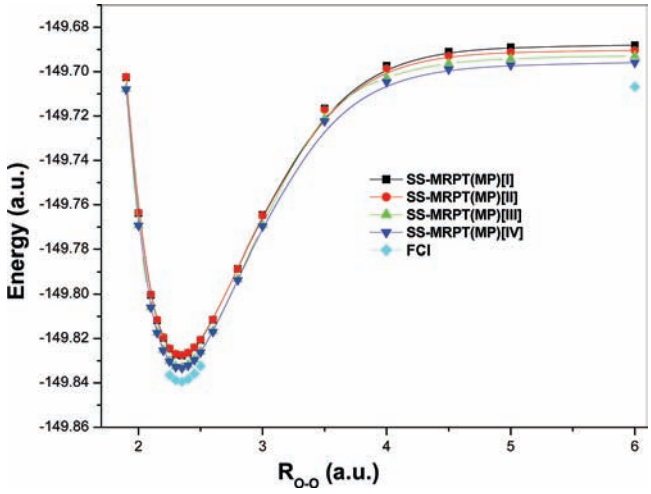

Figure 2. Plot of the dissociation potential energy curves of the lowest singlet delta state ($a^1\Delta_g$) of the O_2 molecule using the DZP basis.

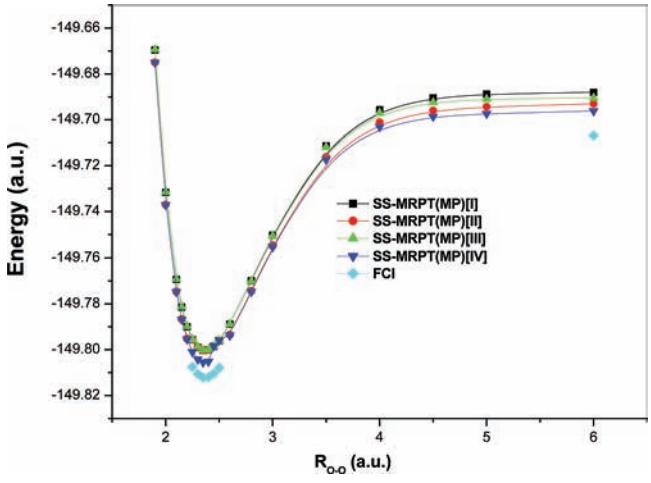

Figure 3. Plot of the dissociation potential energy curves of the lowest singlet sigma state ($b^1\Sigma_g^+$) of the O_2 molecule using the DZP basis.

equilibrium are larger than that in the region of dissociation since more electrons are closer together near equilibrium than at the dissociation limit; the degree of dynamical correlation is larger there and so are the CASSCF errors. From the tables, it is observed that the SS-MRPT(MP) errors are much smaller than the CASSCF errors. The high accuracy of the SS-MRPT(MP) results and the lower NPE values compared to the underlying CASSCF results clearly demonstrate the significance of a well-balanced description of the nondynamical as well as dynamical correlation in the computation of PECs.

It is important to mention the fact that, experimentally,[35] we have observed that the $^3\Sigma_g^-$, $a^1\Delta_g$, and $b^1\Sigma_g^+$ states are approaches toward a near- (or quasi)-degenerate situation with an increasing O−O bond distance beyond the equilibrium position. The CASSCF dissociation potential energy curves for the above-mentioned three states are shown in Figure 4. Although the CASSCF potential energy curves are significantly higher in energy than the exact FCI curve (because of the limited treatment of electron correlation), from the figures, it is clear that all three states considered here provide qualitatively correct PECs and hence can be considered as reasonable starting functions which can be further improved by multireference theory of dynamical correlation, say SS-MRPT(MP) theory. The CASSCF PECs show correct degenerate behavior in the region of dissociation [as the CASSCF is very effective to provide a good and reliable description of electronic near-degeneracies (nondynamical correlation)]. The near-degeneracy behavior of the three electronic states computed via SS-MRPT(MP) and MRMPPT methods is described in Figures 5 and 6. We have observed that the overall performance of the SS-MRPT(MP)[III] is slightly better and more consistent than the other three partitions; in Figure 5, we have only displayed the results obtained by the SS-MRPT(MP)[III] scheme. The three states computed via SS-MRPT(MP)[III] remain very close in energy as they approach the dissociation limit, as is evident from Figure 5. All of the SS-MRPT(MP) states approach the same asymptotic limit and are virtually degenerate. We have mentioned earlier that the performance of the SS-MRPT(MP) method deteriorates to some extent under such circumstances. We should say that more tests and analyses are needed to make a firm judgment on such behavior of the method. The SS-MRPT(MP) and MRMPPT curves are very close to the FCI curve, and they have the correct shape. These methods are accurate enough with respect to the FCI curve. To depict the comparative behavior of the SS-MRPT(MP) and MRMPPT methods, dissociation PECs of the methods as a function of bond length are presented in Figure 6. Among different SS-MRPT(MP) schemes, the Fock operator of SS-MRPT(MP)[III] is structurally close to the Fock operator used in the MRPTMP method. For this reason, we have presented the results of the SS-MRPT(MP)[III] in Figure 6 along with the MRMPPT ones. Figure 6 indicates that the overall performance of these two approaches for the ground state over a wide range of geometries is very close, and the results of the SS-MRPT(MP)[III] and MRMPPT are superimposed on one another around the equilibrium region. For the excited state $a^1\Delta_g$, the SS-MRPT(MP)[III] and MRMPPT methods show almost identical behavior, as is evident from Figure 6.

The first excited singlet delta state has two spatial components (A_g and B_{1g} in D_{2h} symmetry), which should be exactly degenerate. Note that only one component of the $a^1\Delta_g$ state has been considered in the above discussion. Figure 7 shows the calculated PECs for the two degenerate components of the first delta state(s) obtained from our SS-MRPT(MP)[III] calculations. The PECs of the two components of the delta states are superimposed on one another.

To get a better feeling regarding the performance of the various variants of SS-MRPT(MP) schemes, more instructive are plots of the deviations or errors of the total electronic energy from the FCI value at a given molecular geometry R and for a given method X [defined as $\Delta E = E_{(\mathrm{Method})} - E_{(\mathrm{FCI})}$] as a function

TABLE 1: Deviation of the SS-MRPT(MP) Total Energies (au) from FCI (10^{-3} au) for the $^3\Sigma_g^-$ State As a Function of Bond Length (au) Using the DZP Basis[34] and Canonical CASSCF Orbitals

R	CASSCF	SS-MRPT(MP) [I]	SS-MRPT(MP) [II]	SS-MRPT(MP) [III]	SS-MRPT(MP) [IV]	FCI (au)
2.25	143.252	0.387	−8.672	3.546	−1.871	−149.87515
2.3	143.172	0.096	−9.119	3.374	−2.06	−149.87695
2.35	143.001	−0.188	−9.552	3.2	−2.256	−149.87669
2.40	142.740	−0.472	−9.979	3.014	−2.47	−149.87474
2.45	142.442	−0.704	−10.346	2.869	−2.648	−149.87147
6.0	108.069	10.572	−1.355	9.529	−2.239	−149.70689
NPEs (kcal/mol)	22.08	6.75	5.64	4.18	2.84	

TABLE 2: Deviation of the SS-MRPT(MP) Total Energies (au) from FCI (10^{-3} au) for the $^3\Sigma_g^-$ State As a Function of Bond Length (au) Using the DZP Basis[34] and Natural CASSCF Orbitals

R	SS-MRPT(MP) [I]	SS-MRPT(MP) [II]	SS-MRPT(MP) [III]	SS-MRPT(MP) [IV]	FCI (au)
2.25	6.861	−1.069	10.053	5.795	−149.87515
2.3	6.5634	−1.521	9.858	5.556	−149.87695
2.35	6.284	−1.948	9.673	5.319	−149.87669
2.40	6.018	−2.356	9.490	5.08	−149.87474
2.45	5.818	−2.689	9.363	4.889	−149.87147
6.0	18.095	8.557	17.188	7.500	−149.70689
NPEs (kcal/mol)	7.70	6.04	4.91	1.64	

TABLE 3: Deviation of the SS-MRPT(MP) Total Energies (au) from FCI (10^{-3} au) for the $a^1\Delta_g$ State As a Function of Bond Length (au) Using the DZP Basis[34] and Canonical SA-CASSCF Orbitals[a]

R	CASSCF	SS-MRPT(MP) [I]	SS-MRPT(MP) [II]	SS-MRPT(MP) [III]	SS-MRPT(MP) [IV]	FCI (au)
2.25	140.938	11.831	12.094	6.422(5.7912)	6.172	−149.8365
2.3	140.536	11.617	11.872	6.243 (5.549)	5.971	−149.83879
2.35	140.425	11.759	12.001	6.431 (5.693)	6.139	−149.83944
2.4	140.057	11.71	11.934	6.437 (5.669)	6.125	−149.83829
2.45	139.623	11.66	11.859	6.45 (5.664)	6.118	−149.83584
2.50	139.128	11.61	11.781	6.472 (5.675)	6.120	−149.83235
6.0	109.138	18.797	16.465	13.906 (12.140)	10.928	−149.70688
NPEs (kcal/mol)	19.95	4.50	2.94	4.80 (4.13)	3.11	

[a] The values in parentheses indicate the corresponding SS-MRPT(MP)[III] values using CASSCF orbitals.

TABLE 4: Deviation of the SS-MRPT(MP) Total Energies (au) from FCI (10^{-3} au) for the $b^1\Sigma_g^+$ State As a Function of Bond Length (au) Using the DZP Basis[34] and Canonical SA-CASSCF Orbitals

R	CASSCF	SS-MRPT(MP) [I]	SS-MRPT(MP) [II]	SS-MRPT(MP) [III]	SS-MRPT(MP) [IV]	FCI (au)
2.25	140.088	11.835	12.019	6.769	6.548	−149.80751
2.3	139.540	11.672	11.842	6.669	6.433	−149.81063
2.35	139.282	11.848	12.001	6.91	6.662	−149.81215
2.4	138.796	11.848	11.978	8.545	6.717	−149.81191
2.45	138.259	11.846	11.951	7.048	11.951	−149.81041
2.50	137.674	11.842	11.919	7.112	11.919	−149.80789
6.00	109.136	18.84	16.428	13.828	10.691	−149.70687
NPEs (kcal/mol)	19.42	4.50	2.88	4.94	3.44	

of bond distance rather than the percentage of the correlation energy recovered since the former (ΔE) is independent of the definition of the uncorrelated reference wave function energy. The ΔE results of our calculations are collected in the Tables 1, 3, and 4 for the $^3\Sigma_g^-$, $a^1\Delta_g$, and $b^1\Sigma_g^+$ states, respectively. Another useful and instructive way to represent the quality of results with respect to the corresponding FCI ones is the nonparallelity errors (NPE). The NPEs are computed as the difference between the maximum and minimum errors along the PEC (NPE = $\max_R[\Delta E_X(R)] - \min_R[\Delta E_X(R)]$), and they provide a measure of how well each method mimics the overall shape of the exact FCI potential energy curve. The NPE provides an indication of the extent of parallelism of the computed PEC via a given method X with respect to the FCI PEC. Tables 1, 3, and 4 report the NPE values computed for the $^3\Sigma_g^-$, $a^1\Delta_g$, and $b^1\Sigma_g^+$ states, respectively, using different SS-MRPT(MP) variants. The errors (with respect to FCI) tabulated in Table 1 demonstrate that the description of the ground electronic state by the SS-MRPT(MP) is clearly better than the other two reported excited states. For the ground state with the SS-MRPT(MP)[II], we envisage a tendency of overestimation in the equilibrium region; however, this is not so at large *R*, and an underestimated value is found.

From Table 1, it has been observed that the errors (with respect to FCI) for SS-MRPT(MP) schemes for the $^3\Sigma_g^-$ state along the PEC increase in general. The SS-MRPT(MP) method with various forms of H_0 maintains a very modest NPE error. From all of the tables, it is clear that all of the partitionings considered here provide quantitatively accurate potential energy curves. Although the error value (ΔE) of the ground state is small for the SS-MRPT(MP) scheme, the NPE value is higher than that for the other SS-MRPT(MP) schemes. We can say that the NPE of the SS-MRPT(MP)[IV] is slightly better among the four schemes reported in Table 1. The errors of the SS-MRPT(MP)[II] values with respect to the FCI are not as good as that of other three schemes. It is found that the SS-MRPT(MP)[III] method gives better and consistent performance compared to the other three schemes.

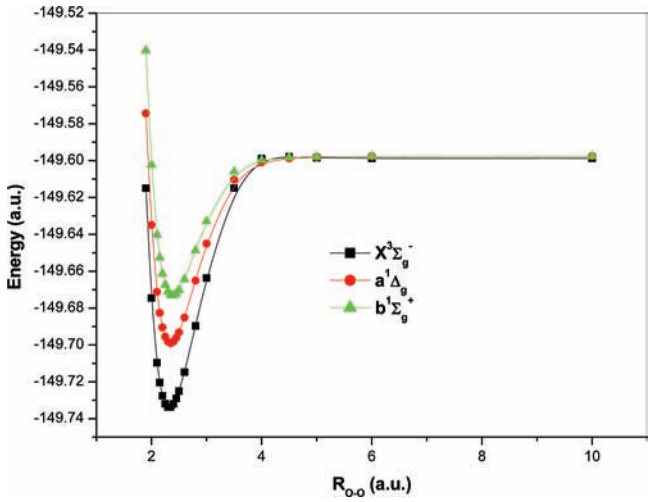

Figure 4. Plot of the CASSCF dissociation potential energy curves of some low-lying states ($^3\Sigma_g^-$, $a^1\Delta_g$, and $b^1\Sigma_g^+$) of the O_2 molecule using the DZP basis.

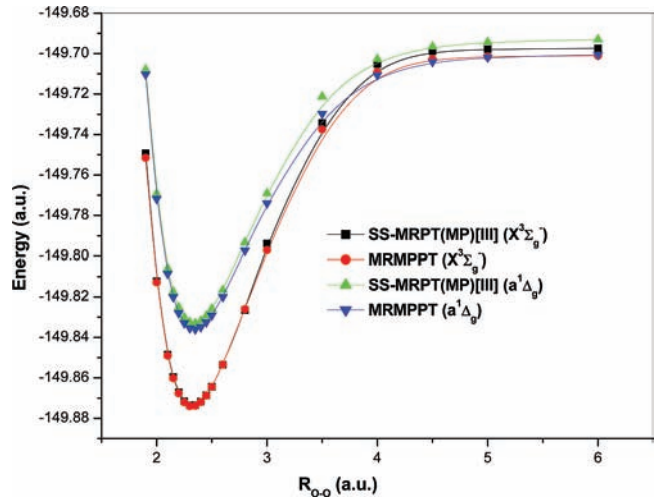

Figure 6. Plot of the SS-MRPT(MP)[III] and MRMPPT dissociation potential energy curves of some low-lying states ($^3\Sigma_g^-$ and $a^1\Delta_g$) of the O_2 molecule using the DZP basis.

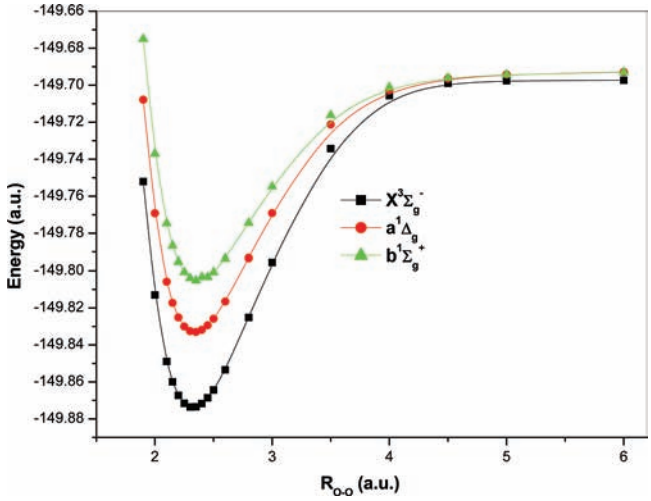

Figure 5. Plot of the SS-MRPT(MP)[III] dissociation potential energy curves of some low-lying states ($^3\Sigma_g^-$, $a^1\Delta_g$, and $b^1\Sigma_g^+$) of the O_2 molecule using the DZP basis.

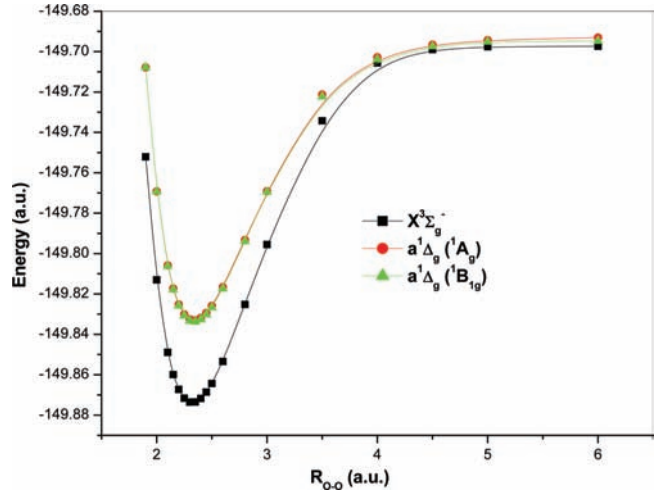

Figure 7. Plot of the SS-MRPT(MP)[III] dissociation potential energy curve of the two components of the $a^1\Delta_g$ state of the O_2 molecule using the DZP basis along with the $^3\Sigma_g^-$ state using the DZP basis.

Table 2 contains the error versus FCI and NPE for the ground state using natural orbitals, which demonstrates the dependence of the results on the nature of orbitals of the perturbative method(s), say SS-MRPT(MP). In this case, the errors are minimum for SS-MRPT(MP)[I] and maximum for SS-MRPT-(MP)[III]. Table 2 demonstrates that over the entire PEC, the SS-MRPT(MP)[I], [III], and [IV] underestimate the state energies with respect to the corresponding FCI values, while SS-MRPT(MP)[II] overestimates the same. The NPE for the ground states of the SS-MRPT(MP) with [I], [II], [III], and [IV] are 7.70, 6.04, 4.91, and 1.64 kcal/mol, respectively. Actually, in both types of orbitals, the overall trend of NPE values of various SS-MRPT(MP) schemes are almost similar. From Table 1, it is observed that the errors of the SS-MRPT(MP)[I] and [III] with respect to the corresponding FCI values increase with the O−O bond elongation. For natural CASSCF orbitals, the accuracy with respect to the FCI values is decreased in the region of dissociation for all partitions. Surprisingly, in the case of canonical CASSCF orbitals, the SS-MRPT(MP)[II] approach shows a minimum deviation in the dissociation limit and maximum error in the region around equilibrium.

From Table 3, we can say that the deviation of SS-MRPT(MP) with respect to the FCI is not large in the case of the $a^1\Delta_g$ as far as excited state is concerned. From a comparison of results in Table 3, we observed that the average deviation (ΔE) is almost identical for SS-MRPT(MP)[I] and SS-MRPT-(MP)[II]. As is apparent from the table of energy differences with respect to the FCI, the computed SS-MRPT(MP)[I] and [II] curves show slightly larger deviations from FCI than those of the SS-MRPT(MP)[III] and SS-MRPT(MP)[IV]. For this excited state, SS-MRPT(MP)[III] and [IV] schemes show almost identical deviation patterns. The NPEs of the SS-MRPT(MP) method with [I], [II], [III], and [IV] are 4.50, 2.94, 4.80, and 3.11 kcal/mol, respectively. As for that of the ground state, the NPEs are also very small in the case of the lowest delta state, $a^1\Delta_g$. The NPEs of SS-MRPT(MP)[III]/[IV] are slightly smaller in comparison to those of the SS-MRPT(MP)[I]/[II]. It is pertinent to note that the state-selective CASSCF reference function of the $a^1\Delta_g$ state would be more accurate than the SA-CASSCF one (especially around equilibrium geometries). For this reason, in Table 3, we have also presented the results using canonical CASSCF orbitals along with SA-CASSCF ones. We have tabulated only the results of the SS-MRPT(MP)[III] scheme (values in parentheses). It is found that the accuracy increases marginally upon using CASSCF orbitals instead of SA-CASSCF ones.

In Table 4, we have tabulated the deviation of the results of the SS-MRPT(MP) method with various H_0 from the corresponding FCI results for the $b^1\Sigma_g^+$ state. As for that of the $a^1\Delta_g$ state, the trend of deviation of the SS-MRPT(MP) method with respect to the FCI is almost identical. The error for the SS-MRPT(MP)[III] and [IV] schemes is small near the equilibrium region which increases as one moves toward the dissociation limit. For the SS-MRPT(MP)[I] and [II] schemes, the difference of the deviation between equilibrium and the dissociation zone is small in comparison to the other two schemes. From this table, we have observed that although the deviation is slightly large (except for the SS-MRPT(MP)[IV]), the NPEs are very small. The NPEs for this state are 4.50, 2.88, 4.94, and 3.44 kcal/mol, respectively.

We have observed that the SS-MRPT(MP)[III] performs better than the corresponding other partitioning schemes for the system studied by us in this article. In the case of the excited state, the average deviations for the various SS-MRPT(MP) approaches remain the same as those in the equilibrium region, whereas upon approaching toward the dissociation limit, the deviation increases slightly as that of the ground state.

Nevertheless, across all four definitions of diagonal H_0(OE) considered in this article, there is a good overall agreement between the FCI state energies and our calculated values. The NPEs of various SS-MRPT(MP) schemes for both the ground as well as excited states are reasonably small. From the point of view of NPEs and FCI error values, we have found that the performance of the SS-MRPT(MP)[III] approach is better and consistent among the four variants. Concluding, the SS-MRPT(MP) schemes describe the region near equilibrium more accurately in comparison to the dissociation region. However, it must be kept in mind that the smaller active space may lead to a relatively unsatisfactory value of deviation, ΔE, in some cases.

The encouraging PECs computed via the SS-MRPT(MP) method for both the ground and the excited states of the O_2 system provide motivation for investigating the spectroscopic constants and their accuracy. The various SS-MRPT(MP) approaches have been applied to the calculation of spectroscopic parameters of the $^3\Sigma_g^-$, $a^1\Delta_g$, and $b^1\Sigma_g^+$ states of the O_2 molecule. We have tabulated the calculated spectroscopic constants along with FCI values (whenever available) and experimental data in Tables 5−10. In Table 5, the values within the parentheses correspond to the values using natural CASSCF orbitals. In addition to FCI and experimental data,[35] results of various ab initio methods have also been reported for comparison. The values of the equilibrium bond length, r_e, and the vibrational frequency ω_e, are generally in very close agreement with the FCI values. From the tables, it is observed that the change of values of the SS-MRPT(MP) method with different versions of diagonal H_0(OE) for the bond length (r_e) and vibrational frequency (ω_e) displays the same trend as that of the FCI ones if one goes from one state to the other.

In the case of the ground-state $^3\Sigma_g^-$ equilibrium distance, r_e, the SS-MRPT(MP)[III] result is better than that of the other three schemes and is comparable to CASPT2 and MRMPPT results. For the $^3\Sigma_g^-$ state, the r_e values of CASPT2 and SS-MRPT(MP) are very close to each other. For the lowest singlet delta state $a^1\Delta_g$, the equilibrium bond lengths obtained by various SS-MRPT(MP) approaches are very close to one another and are comparable to the MRMPPT value. In comparison to the FCI values, the various SS-MRPT(MP) schemes describe the equilibrium bond length very well in the case of the lowest singlet sigma state, $b^1\Sigma_g^+$.

TABLE 5: Spectroscopic Constants for $^3\Sigma_g^-$ of O_2 (r_e in Å, D_e in eV, and ω_e in cm^{-1}) Using the DZP basis,[34] the cc-pvTZ Basis, and CASSCF Canonical Orbitals[a]

basis	method	r_e	ω_e	D_e
DZP	CASSCF	1.2291 (1.2288)	1606 (1606)	3.68 (3.68)
	SS-MRPT(MP)[I]	1.2316 (1.2305)	1593 (1571)	4.91 (4.95)
	SS-MRPT(MP)[II]	1.2325 (1.2326)	1649 (1562)	4.82 (4.85)
	SS-MRPT(MP)[III]	1.2292 (1.2292)	1643 (1573)	4.82 (4.90)
	SS-MRPT(MP)[IV]	1.2295 (1.2326)	1640 (1567)	4.66 (4.70)
	MRMPPT	1.2298	1568	4.71
	Roos[b] CASPT2D	1.2280	1607	4.70
	CASPT2N	1.2260	1607	4.65
	FCI	1.227	1642	4.64
cc-pVTZ	CASSCF	1.2167	1535	3.92
	SS-MRPT(MP)[I]	1.2191 (1.2146)	1542 (1583)	5.34 (5.25)
	SS-MRPT(MP)[II]	1.2221 (1.2171)	1526 (1570)	5.17 (5.05)
	SS-MRPT(MP)[III]	1.2179 (1.2136)	1544 (1583)	5.18 (5.13)
	SS-MRPT(MP)[IV]	1.2190 (1.2136)	1530 (1583)	4.91 (4.86)
	CCSD[c]	1.199	1679.1	
	CCSD(T)[c]	1.211	1589.6	
	4R-BWCCSD[c]	1.199	1683	
	4R-MkCCSD[c]	1.198	1686.6	
	4R-BWCCSD(T)[c]	1.2129	1577.4	
	4R-MkCCSD(T)[c]	1.2121	1582.1	
	8R-BWCCSD(T)[c]	1.2129	1576.7	
	8R-MkCCSD(T)[c]	1.2121	1582.1	
	8R-CISD[c]	1.198	1670.1	
	experiment[d]	1.2075	1580	5.21

[a] The values in parentheses indicate the SS-MRPT(MP) values for natural orbitals. [b] Reference 34. [c] Reference 32. [d] Experiment: ref 35.

TABLE 6: Spectroscopic Constants for $^3\Sigma_g^-$ of O_2 (r_e in Å, D_e in eV, and ω_e in cm^{-1}) Using the cc-pvQZ Basis

basis	method	r_e	ω_e	D_e
cc-pVQZ	SS-MRPT(MP)[III]	1.2146	1553	5.32
	4R MkCCSD[a]	1.1943	1700.1	
	4R BWCCSD(T)[a]	1.2091	1589.6	
	4RMkCCSD(T)[a]	1.2084	1594.3	
	8R MkCCSD[a]	1.1943	1700.1	
	8R BWCCSD(T)[a]	1.2091	1589.7	
	8R MkCCSD(T)[a]	1.2084	1594.3	
	experiment[b]	1.2075	1580	5.21

[a] Reference 32. [b] Experiment: ref 35.

TABLE 7: Spectroscopic Constants for $^3\Sigma_g^-$ of O_2 (r_e in Å, D_e in eV, and ω_e in cm^{-1}) Using the DZP basis[36] [Van Dam et al.][a]

method	r_e	ω_e	D_e
SS-MRPT(MP)[III]	1.2287	1596	4.70
MRMPPT	1.2284	1601	4.54
Werner[b] CASPT2	1.2126	1566.1	5.12
CASPT3	1.2076	1590.9	4.89
Andersson[b] CASMP2	1.2117	1585.4	5.31
CASMP3	1.2063	1584.0	4.95
Wolinski[b] CASMP2	1.2116	1587.7	5.31
CASMP3	1.2069	1579.6	4.93
Dam[b] CASMP2	1.2127	1587.2	5.33
CASMP3	1.2070	1583.9	4.89
experiment[c]	1.2075	1580	5.21

[a] Canonical CASSCF orbitals are used SS-MRPT(MP[III] and MRMTPT calculations. [b] Reference 36. [c] Experiment: ref 35.

Table 5 clearly demonstrates that the vibrational frequency ω_e for the ground state computed via SS-MRPT(MP) approaches are very close to the corresponding FCI value. From the table, we have seen that the ω_e value of CASPT2 is closer to the FCI than the SS-MRPT(MP) value. In the case of $a^1\Delta_g$, the performance of the SS-MRPT(MP) method with various forms of diagonal H_0(OE) to compute the vibrational frequency is almost identical. For the $b^1\Sigma_g^+$ state, the situation is very similar,

TABLE 8: Spectroscopic Constants for $a^1\Delta_g$ and $b^1\Sigma_g^+$ States of O_2 Using the DZP Basis[34] (r_e in Å, D_e in eV, and ω_e in cm^{-1})[a]

states	basis	method	r_e	ω_e	D_e
$a^1\Delta_g$	DZP	CASSCF	1.2434	1425	2.75
		SS-MRPT(MP)[I]	1.2387	1455.57	3.80
		SS-MRPT(MP)[II]	1.2390	1453.3	3.73
		SS-MRPT(MP)[III]	1.2379	1459.6	3.81
			(1.2379)	(1496)	(3.80)
		SS-MRPT(MP)[IV]	1.238	1459.6	3.74
		MRMPPT	1.2412	1463.6	3.68
		FCI	1.234	1539	3.61
		experiment[b]	1.2155	1509.3	
$b^1\Sigma_g^+$	DZP	CASSCF	1.2621	1263	2.05
		SS-MRPT(MP)[I]	1.2528	1438.8	3.06
		SS-MRPT(MP)[II]	1.2531	1436.0	2.99
		SS-MRPT(MP)[III]	1.2518	1439.6	3.06
		SS-MRPT(MP)[IV]	1.2518	1439.7	2.98
		FCI	1.2532	1517.0	2.87
		experiment[b]	1.2267	1432.6	

[a] The values in parentheses describe the values using CASSCF orbitals instead of SA-CASSCF. [b] Experiment: ref 35.

TABLE 9: Spectroscopic Constants for the $a^1\Delta_g$ State of O_2 Using cc-pVTZ and cc-pVQZ Basis Sets[37] (r_e in Å, D_e in eV, and ω_e in cm^{-1})

basis	method	r_e	ω_e	D_e
cc-pVTZ	CASSCF	1.2302	1440	3.00
	SS-MRPT(MP)[III]	1.2256	1460	4.23
	4R-BWCCSD[a]	1.204	1628.4	
	4R-MkCCSD[a]	1.2049	1627.1	
	4R-BWCCSD(T)[a]	1.2193	1523.2	
	4R-MkCCSD(T)[a]	1.2147	1539.5	
	8R-BWCCSD(T)[a]	1.2165	1520.6	
	8R-MkCCSD(T)[a]	1.2161	1528.1	
	8R-CISD[a]	1.208	1583.0	
cc-pVQZ	SS-MRPT(MP)[III]	1.2203	1471	4.40
	4R-MkCCSD[a]	1.2001	1645.3	
	4R-BWCCSD(T)[a]	1.2147	1539.5	
	4R-MkCCSD(T)[a]	1.2148	1539.0	
	8R-MkCCSD[a]	1.2016	1632.5	
	8R-BWCCSD(T)[a]	1.2165	1520.6	
	8R-MkCCSD(T)[a]	1.2161	1528.1	
	experiment[b]	1.2155	1509.3	

[a] Reference 32. [b] Experiment: ref 35.

as can be seen for the $a^1\Delta_g$ state. At the SS-MRPT(MP) level, the ω_e values are overestimated for all of the states with respecte to the experimental values as in the case of r_e results. A similar feature is also present in FCI calculations.

We now discuss the potential of the SS-MRPT(MP) method to provide dissociation energy using various diagonal H_0(OE) schemes. The quality of the values obtained for the dissociation energy is very sensitive with respect to the complete treatment of the correlation energy. Table 8 demonstrates that the performance of the SS-MRPT(MP) for the ground state to compute the dissociation energy is very modest and close to the FCI value. The quality of the SS-MRPT(MP) dissociation energy using canonical and natural CASSCF orbitals [values in the parentheses in the Table 8] is almost identical. The CASSCF dissociation energy is too low. For the $a^1\Delta_g$ and $b^1\Sigma_g^+$ state, the dissociation energy generated via various variants of the SS-MRPT(MP) methods show a similar behavior, and the results are very encouraging with respect to the FCI value. As Table 8 shows, for the $^3\Sigma_g^-$, $a^1\Delta_g$, and $b^1\Sigma_g^+$ states, the D_e is also overestimated by the SS-MRPT(MP) methods. Across all of the states, although the SS-MRPT(MP) methods overestimate

TABLE 10: Spectroscopic Constants for the $b^1\Sigma_g^+$ State of O_2 Using cc-pVTZ and cc-pVQZ Basis Sets[37] (r_e in Å, D_e in eV, and ω_e in cm^{-1})

basis	method	r_e	ω_e	D_e
cc-pVTZ	CASSCF	1.2485	1368	3.28
	SS-MRPT(MP)[III]	1.2381	1412	3.49
	4R-BWCCSD[a]	1.211	1576.1	
	4R-MkCCSD[a]	1.2126	1570.3	
	4R-BWCCSD(T)[a]	1.2242	1472.7	
	4R-MkCCSD(T)[a]	1.2252	1465.6	
	8R-BWCCSD(T)[a]	1.2304	1426.8	
	8R-MkCCSD(T)[a]	1.2293	1437.6	
	8R-CISD[a]	1.220	1496.9	
cc-pVQZ	SS-MRPT(MP)[III]	1.2319	1425	3.65
	4R-MkCCSD[a]	1.2071	1591.4	
	4R-BWCCSD(T)[a]	1.2242	1472.7	
	4R-MkCCSD(T)[a]	1.2252	1465.6	
	8R-MkCCSD[a]	1.2106	1568.6	
	8R-BWCCSD(T)[a]	1.2304	1426.8	
	8R-MkCCSD(T)[a]	1.2293	1437.6	
	experiment[b]	1.2267	1432.6	

[a] Reference 32. [b] Experiment: ref 35.

the D_e value, they, however, give reasonable values. Table 8 depicts that the D_e values of the MRMPPT and SS-MRPT(MP) are very close to one another.

In our application, we have also quoted the excitation energies for $^3\Sigma_g^- \rightarrow a^1\Delta_g$ as well as $^3\Sigma_g^- \rightarrow b^1\Sigma_g^+$. The results are reported in Table 12 states. From the table, it is clear for ΔE_1 and ΔE_2 that the value computed via SS-MRPT(MP)[I] is closer to the corresponding FCI values than those of the other SS-MRPT(MP) schemes. Actually, the quality of results provided by SS-MRPT(MP)[I] is quite encouraging. In the case of ΔE_1, the value generated via SS-MRPT(MP)[II] is closer to the FCI value than that for the ΔE_2 one. At this point, we want to make a comment that, on average, the SS-MRPT(MP) does not lead to accurate excitation energies in general. From the table, it is also clear that this lack of accuracy has not changed significantly by the use of different forms of diagonal MP H_0, that is, H_0(OE). Despite the drastic simplification of the SS-MRPT(MP), our results of excitation energy are encouraging.

To establish the applicability of SS-MRPT(MP) approaches, we have presented the spectroscopic constants using the same basis and scheme as that of Van Dam et al.[36] in Table 7 along with the results of various CAS-based MP2/MP3 methods.[34,36] From the foregoing analysis, we have already noticed that the performance of SS-MRPT(MP)[III] is marginally better than that of the other three. For this reason, we depict only the results corresponding to the SS-MRPT(MP)[III] scheme. The ground-state r_e values of the CASMP2 methods are closer to the experimental result than those of the SS-MRPT(MP)[III] method. For all of the states considered here, the r_e values computed via the SS-MRPT(MP)[III] scheme and various CAS-based MP2 methods are slightly larger than the experimental values. For the ground state, the r_e values of CASMP3 are closer to the experimental result. In the case of the r_e value for the $^3\Sigma_g^-$ state, the performance of MRMPPT and the SS-MRPT-(MP)[III] are very close to one another.

The overall performance of the SS-MRPT(MP) to provide the ω_e value resembles closely the various CASMP2 as well as CASMP3 values. It is noted that the computational cost of MP3 is higher than the corresponding MP2 calculations. For the computation of ω_e, the MRMPPT method shows slightly better performance than the other perturbative methods reported in Table 7, including SS-MRPT(MP)[III].

For the ground state, from Table 5, it is found that the D_e values of various CAS-based MP2 methods are higher than the SS-MRPT(MP)[III] values with respect to the experimental value. On the other hand, the D_e values for the ground state provided by various CASMP3 are close to the SS-MRPT-(MP)[III] value. It is also observed that, for the dissociation energy, D_e, the SS-MRPT(MP)[III] performs better than the MRMPPT approach with respect to the experimental value.

It should be noted that a comparison of the quality of various spectroscopic parameters generated via different many-body methods using the DZP basis with the FCI value is physically more meaningful than comparison with corresponding experimental ones. As the DZP basis is too small for a meaningful comparison with experimental results, in this paper, we have also performed calculations of the ground and excited states' spectroscopic constants using cc-pVTZ and cc-pVQZ basis sets.[37] The corresponding spectroscopic results for the ground state are tabulated in Tables 5 and 6. Since FCI calculations are unfeasible for such a large system and basis sets, the quality of the spectroscopic constants generated via the various SS-MRPT(MP) schemes is calibrated through comparison with the spectroscopic data obtained using recently developed and well-tested techniques. For this purpose, we have tabulated cc-pVTZ results of MR-BWCCSD, MR-BWCCSD(T), MR-MkCCSD, MR-MkCCSD(T), CISD, and so on. It was observed that the quality of the equilibrium distance and dissociation energy generally improves with an increase in the size of the basis. The equilibrium distances obtained with SS-MRPT(MP) are found to be as accurate as full-blown MRCCSD(T) values, while the equilibrium distances computed by CCSD, 8R-CISD, 4R-MkCCSD, and 4R-BWCCSD are somewhat slightly small with respect to the experimental value. The increase of the size of the basis set (i.e., of the basis set quality) leads to an increase in the quality of the equilibrium bond distance with respect to the experimental value. Thus, the effect of basis sets on the value of the SS-MRPT(MP) equilibrium bond distance is generally converging in nature. These results reconfirm the applicability and efficacy of the SS-MRPT(MP) method. In the case of the vibrational frequency, the values provided by the four variants of the SS-MRPT(MP) approaches are closer to the experimental one for the cc-pVTZ basis than that of the DZP basis. We also notice that for the cc-pVTZ basis, the accuracy of the vibrational frequency provided by SS-MRPT(MP) schemes is better than that of the CCSD, CCSD(T), 4R-BWCCSD, and 4R-MkCCSD approaches, although the numerical implementation of the CC method is computationally quite demanding with respect to the SS-MRPT(MP) one. For the cc-pvTZ basis, the SS-MRPT(MP) vibrational frequency is very close to the 8R-BWCCSD(T) and 8R-MkCCSD(T) ones, despite the fact that the computational cost of MRCCSD(T) methods is quite high compared to the SS-MRPT(MP) one. Interestingly, the results for the dissociation energies for cc-pVTZ basis are the cases in which the SS-MRPT(MP)[I], [II], and [III] are in better agreement with the experimental values than the DZP basis set. Table 6 illustrates that the cc-pVQZ basis yields improved spectroscopic constants. A switch-over to a larger basis set shows that the improvement of the quality of dissociation energy and vibrational frequency with respect to the corresponding experimental values is again satisfactory as that of the equilibrium bond distance. From our foregoing discussion, we may claim that the performance of the SS-MRPT(MP) method is comparable in accuracy to the full-blown MRCCSD and MRCCSD(T) methods. Note that the MRCC methods usually suffer from a great complexity of working equations and severe computational costs compared to the corresponding MRPT scheme.

While the SS-MRPT(MP) scheme has given encouraging results using the DZP basis in the computation of dissociation PECs of the low-lying excited states, $a^1\Delta_g$ and $b^1\Sigma_g^+$ of the oxygen molecule, it has not yet been used by us in conjunction with large basis sets. To demonstrate the importance of using large basis sets to assess the accuracy of the SS-MRPT(MP) results for these states, we have also applied the method to extract spectroscopic constants from the dissociation PECs for the cc-pVTZ basis. For example, Tables 9 and 10 describe the excited-state ($a^1\Delta_g$ and $b^1\Sigma_g^+$) spectroscopic properties of O_2 computed at the SS-MRPT(MP), CISD, BWCC, and Mk-MRCC levels and various other methods using the cc-pVTZ basis sets together with the experimental values which help us to calibrate the computed results. The tables show that 8R-CISD, 4R-BWCCSD, and 4R-MkCCSD intrinsically underestimate the O−O bond length, while CASSCF and SS-MRPT(MP)[III] overestimate it. From Tables 8−10, we have found that the equilibrium O−O bond distance generated via SS-MRPT(MP) moves toward the experimental value as one moves from the DZP basis to the cc-pVTZ basis. In the case of the delta state, the SS-MRPT(MP) equilibrium O−O bond distance is closer to the experimental values than that of the 8R-CISD one, whereas for the lowest singlet sigma state, the result of 8R-CISD is better than that of our SS-MRPT(MP) result.

Tables 9 and 10 clearly demonstrate that the quality of the vibrational frequency is also improved as we increase the size of the basis sets. The vibrational frequencies show a behavior similar to that of r_e. Tables 9 and 10 show that all of the methods mentioned here overestimate the vibrational frequency in comparison to the experimental value, except for the CASSCF method. In the case of the $a^1\Delta_g$ state, among the various methods tabulated here, the SS-MRPT(MP) prediction for the vibrational frequency is the closest to the experimental value. While this success does not appear to be fortuitous, more studies using various basis sets (with values extrapolated to the complete basis set limit) are required to determine if such agreement is a general occurrence. For the $b^1\Sigma_g^+$ state, the performance of SS-MRPT(MP) to provide ω_e is better than that of the 8R-CISD, 4R-MkCCSD, 4R-BWCCSD, 4R-BWCCSD(T), and 4R-MkCCS-D(T) methods. In summary, MkCCSD(T) provides excellent results for r_e and ω_e of O_2 and is superior to the other methods reported here. From Tables 9 and 10, not only r_e and ω_e but the SS-MRPT(MP) theory is also able to predict an accurate dissociation energy for the lowest singlet delta and excited singlet sigma states with the cc-pVTZ basis set as compared to experiment.

The spectroscopic data in Tables 5, 6, and 8−10 show the necessity of using large basis sets in assessing intrinsic errors for the SS-MRPT(MP) method. Generally, for all methods discussed in this paper, the values of accuracy of spectroscopic constants increase significantly in going from the DZP to the cc-pVTZ basis set with respect to the experimental values. The results in Tables 5, 6, and 8−10 support the accuracy and reliability of SS-MRPT(MP) when compared to the recently developed full-blown Mukherjee's and Brillouin−Wigner state-specific multireference coupled-cluster results. In summary, the SS-MRPT(MP) method provides substantially encouraging results for the various spectroscopic parameters. To get a feeling at a glance, in Table 11, we have summarized the effect of basis sets size on various spectroscopic constants of the SS-MRPT-(MP)[III] method. Table 11 clearly illustrates the improvement

TABLE 11: Spectroscopic Constants of O_2 using the SS-MRPT(MP)[III] Approach and Various Basis Sets[37] (r_e in Å, D_e in eV, and ω_e in cm^{-1})

state	basis	r_e	ω_e	D_e
$^3\Sigma_g^-$	DZP	1.2307	1565	4.80
	cc-pVTZ	1.2179	1544	5.18
	cc-pVQZ	1.2146	1553	5.32
	experiment[a]	1.2075	1580	5.21
$a^1\Delta_g$	DZP	1.2390	1453.3	3.73
	cc-pVTZ	1.2256	1460	4.23
	cc-pVQZ	1.2203	1471	4.40
	experiment[a]	1.2155	1509.3	
$b^1\Sigma_g^+$	DZP	1.2531	1436.0	2.99
	cc-pVTZ	1.2381	1412	3.49
	cc-pVQZ	1.2319	1425	3.65
	experiment[a]	1.2267	1432.6	

[a] Experiment: ref 35.

TABLE 12: Excitation Energies (eV) for Two Low-Lying Singlet Excited States of O_2 along with the FCI Results Using the DZP basis[34] [$\Delta E_1 = E_{^3\Sigma_g^-}(R_{eq}) - E_{a^1\Delta_g}(R_{eq})$ and $\Delta E_2 = E_{^3\Sigma_g^-}(R_{eq}) - E_{b^1\Sigma_g^+}(R_{eq})$]

basis	method	ΔE_1	ΔE_2
DZP	SS-MRPT(MP)[I]	1.3439	2.087
	SS-MRPT(MP)[II]	1.1086	1.856
	SS-MRPT(MP)[III]	1.6041	2.344
	SS-MRPT(MP)[IV]	1.2487	2.004
	FCI	1.082	1.823

of the basis set in bringing the spectroscopic constants into better agreement with experiment.

In the above analysis, we have utilized the SS-MRPT(MP) method with different partitioning schemes to describe bond breaking of the O_2 molecule in the ground electronic state, as well as that in other low-lying excited states of the different spin symmetry by extrapolating different basis sets. We have also presented the spectroscopic constants using computed PECs via the SS-MRPT(MP) method with different partitioning schemes. The smoothness of the results of the PECs and spectroscopic constants gave us confidence on the SS-MRPT(MP) to calculate the vertical excitation energy. The quality of the computed PECs can also be judged from the calculated excitation energies. The $b^1\Sigma_g^+$ state has a much shorter lifetime than the $a^1\Delta_g$ state because $b^1\Sigma_g^+$ is more reactive than the $a^1\Delta_g$ form. It decays to the $a^1\Delta_g$ state before chemical reactions can occur. The computation of the vertical excitation energy is a very challenging task from a theoretical point of view since to get correct result, a proper and balanced description of the states involved is necessary. Thus, the study of the energy gap of these singlet states with respect to the ground states makes a challenging and interesting target for theoretical studies. The vertical excitation energy for the states' $X^3\Sigma_g^- \rightarrow a^1\Delta_g$ and $X^3\Sigma_g^- \rightarrow b^1\Sigma_g^+$ transition of oxygen computed via the SS-MRPT(MP) method is investigated and compared with the results generated using high-level theoretical methods also provided in this paper. In our calculation, vertical excitation energies (T_e) were calculated at the equilibrium interatomic distance[35] of the ground state. The vertical excitation energy is more physical than the excitation energy reported in Table 12. Vertical excitation energies using DZP cc-pVTZ and cc-pVQZ basis sets are listed in Table 13 along with other available results.[32] Although we have not studied the calculations up to the basis set saturation limit, for the sake of completeness of comparison, we have tabulated the corresponding experimental values. As we have already observed that the results of the SS-MRPT(MP)[III] are better than those of the other SS-MRPT(MP) schemes, we depict here only the results corresponding to the SS-MRPT(MP)[III]. Results of SS-MRPT(MP) significantly overestimated both transition energies for all three basis sets considered here. It is seen that the deviation of $T_e(1)$ computed using SS-MRPT(MP) increases, and that of $T_e(2)$ decreases with respect to the experimental value if one goes from the DZP to cc-pVTZ basis. On the other hand, comparison with experimental data indicates that the calculation with larger basis set, say cc-pvQZ, shows that the accuracy improves. From the table, we may say that the performance of the SS-MRPT(MP) method to compute the vertical energy of a complex system like oxygen is very encouraging. The lack of accuracy to compute vertical excitation energies via different methods reported here is due to the fact that the more accurate description of dynamical correlation has a larger effect for the ground state than that for the two excited states. The extensions of model space and of the basis set may lower the vertical excitation energy. We feel that the performance of the SS-MRPT method needs to be studied in greater detail in the future.

TABLE 13: Vertical Excitation Energies (eV) for Two Low-Lying Singlet Excited States of O_2 Using DZP,[34] cc-pVTZ, and cc-pVQZ[37] Basis Sets [$T_e(1) = E_{^3\Sigma_g^-} - E_{a^1\Delta_g}$ and $T_e(2) = E_{^3\Sigma_g^-} - E_{b^1\Sigma_g^+}$]

basis	method	$T_e(1)$	$T_e(2)$
DZP	SS-MRPT(MP)[III]	1.105	1.870
cc-pVTZ	SS-MRPT(MP)[III]	1.122	1.850
	DIP-STEOM-CCSD[a]	1.066	1.803
	8R-CISD[a]	0.982	1.698
	4R-BWCCSD[a]	1.058	1.902
	4R-RSCCSD[a]	1.033	1.852
	4R-MkCCSD[a]	0.995	1.790
	4R-BWCCSD(T)[a]	1.093	1.848
	4R-MkCCSD(T)[a]	1.030	1.736
	8R-BWCCSD[a]	1.026	1.777
	8R-RSCCSD[a]	1.006	1.760
	8R-MkCCSD[a]	0.973	1.701
	8R-BWCCSD(T)[a]	1.074	1.774
	8R-MkCCSD(T)[a]	1.016	1.671
cc-pvQZ	SS-MRPT(MP)[III]	1.104	1.829
	4R-BWCCSD	1.035	1.876
	4R-RSCCSD	1.013	1.831
	4R-MkCCSD	0.974	1.766
	4R-BWCCSD(T)	1.074	1.826
	4R-MkCCSD(T)	1.008	1.708
	8R-BWCCSD	1.004	1.754
	8R-RSCCSD	0.985	1.736
	8R-MkCCSD	0.950	1.674
	8R-BWCCSD(T)	1.050	1.747
	8R-MkCCSD(T)	0.993	1.640
	experimental[b]	0.982	1.636

[a] Reference 32. [b] Experiment: ref 35.

It is well stated now that the approaches based on Mukherjee's SSMR method[27] have a difficulty for accurately modeling bond-breaking or bond-forming processes (i.e., for computing dissociation PECs) since they are incapable of properly describing degeneracies among electron configurations if the state of interest is not well separated from the virtual states functions (i.e., has no intruder itself). This fact may lead to some inaccuracy while computing energies over a wide range of geometries and hence spectroscopic constants including the vertical excitation energy. The ground state is often well separated from the excited states of a molecule, at least close to the equilibrium geometry, while different excited states can be close in energy. When we compute energy curves at

geometries away from equilibrium, we often find crossing energy curves with a change of dominating electronic configurations.

It is needless to say that to achieve a higher degree of accuracy for PECs and spectroscopic constants, use of other sophisticated ab initio methods, say, MRCC or MRCEPA (coupled electron pair approximation)-like methods, are called for. However, the computational expense of CC methods is significantly greater than that of the MPPT methods at the same excitation rank. For many systems, such as the oxygen molecule, it has been found that it is necessary to compute the dynamical correlation at a higher level than with only the connected singles−doubles level of approximation of the cluster operator. Very recently, Pittner and co-workers[32] have shown that the triexcitations have a large effect on the state energies and spectroscopic constants of the first three electronic states for the oxygen molecule, and they showed that the results obtained using MR-MkCCSD(T) [the SS-MRCC method of Mukherjee and co-workers[7] with connected singles, doubles, and perturbative triples (which play a significant role in reducing errors)] are in good agreement with the experimental data as CC methods treat electron correlation more efficiently than the corresponding perturbative methods.

IV. Summarizing Remarks

The calculations in this paper have been carried out in order to examine the performance of a spin-free version of the size-extensive SS-MRPT(MP) method of Mukherjee and co-workers for the description of PECs of the open-shell molecule. This method is especially important when one encounters near-degeneracies and the effect of intruders. The SS-MRPT method addresses the solution of specific states of interest one at a time and is thus free from the intruder state problem as long as the target state is well separated from the virtual one. In this work, we have applied the method to bond breaking of oxygen molecule using different basis sets. Several reasonable choices of the one-particle unperturbed Hamiltonian H_0 in the Møller−Plesset (MP) partitioning for the SS-MRPT(MP) have been considered, and the quality of the corresponding results have been illustrated and discussed. The SS-MRPT(MP) theory is a computationally economical method which can provide very encouraging results for the bond-breaking problem considered here.

In this article, we have studied the low-lying energy spectrum [ground state, $X^3\Sigma_g^-$, as well as first two singlet excited states, $a^1\Delta_g$, and $b^1\Sigma_g^+$] of the oxygen molecule using the various variants of the SS-MRPT(MP) in order to demonstrate the efficiency of the method. Besides calculating the ground- and several excited-state energies, we have also obtained spectroscopic data and vertical excitation energies as well. The dissociation of the O_2 molecule is a serious test for a method aimed at calculating PECs. The computed results of the PECs via various SS-MRPT(MP) schemes are compared with FCI values and other methods whenever available. The computed SS-MRPT(MP) results of the state energies for all bond lengths (across the entire PECs) have been obtained with good accuracy for the ground and two lowest singlet excited states of the oxygen molecule. The error curves show that the ground state generated via SS-MRPT(MP) is generally better than the other two excited states. To demonstrate the efficacy of the SS-MRPT(MP) method, we have also computed the NPEs. From our computed NPE indices, we have observed that the SS-MRPT(MP) approaches with various diagonal H_0(OE) are quite competitive. For spectroscopic constants, comparisons with experimental data are also made as a final measure of the performance of the SS-MRPT(MP) method. It is demonstrated that the performance of the SS-MRPT(MP) with different diagonal H_0(OE) is very modest at moderate computational cost in predicting state energies across the PEC, structure, and vibrational frequency. For the ground state, the accuracy of the spectroscopic constants of the SS-MRPT(MP) method is comparable to that of the results of the BWCCSD(T) and MkCCSD(T) methods. The different variants of SS-MRPT(MP) provide more accurate spectroscopic results than those obtained with the CCSD for the ground state. Actually, the values of the spectroscopic constants of the ground as well as some low-lying excited states computed with the SS-MRPT(MP) using different H_0 indicate that they also fare pretty well. Although we have not studied the performances of SS-MRPT(MP) methods up to the basis set saturation limit, comparison with experimental data indicates that the values of the various spectroscopic constants improve with the increase in size of the basis set. We have observed that for a number of choices of diagonal H_0(OE), the equilibrium distances, vibrational frequency, and dissociation energy obtained via SS-MRPT(MP) are of similar accuracy, on average, for a given state. With the example application discussed here, it seems to us that the performance of the SS-MRPT(MP)[III] scheme is generally better than the other partitions. A numerical test of different versions of SS-MRPT(MP) approaches in this paper demonstrate their accuracy in excited-state calculations in rather complicated situations such as the two lowest singlet excited states of an oxygen molecule containing quasi-degenerate electronic configurations of varying weight across the entire PEC. We have demonstrated numerically that the SS-MRPT(MP) has the ability to yield results (of PECs and spectroscopic constants including vertical excitation energy) of reasonable accuracy for O_2, a well-known challenging target for theoretical studies. The equilibrium distances, harmonic frequencies, dissociation energies for various states, and vertical excitation energies obtained with SS-MRPT(MP) are found to be as accurate as other MRMP and MkMRCC and BWMRCC values. Particularly accurate results are obtained when higher-order correlation of all electrons along with larger basis sets and model space are considered. While the present analysis aimed essentially at revealing the applicability and accuracy of different variants of SS-MPR(MP) to study the ground and low-lying electronic states of the oxygen molecule, it also gave rise to a practically valuable tool for singlet and nonsinglet molecular electronic state computations.

Acknowledgment. We are grateful to the anonymous referee for his critical remarks and suggestions. This work has been supported by the Department of Science and Technology (DST), India [Grant No.SR/S1/PC-32/2005]. We also wish to acknowledge the help of Debi Banerjee in preparing the manuscript.

References and Notes

(1) (a) Møller, C.; Plesset, M. S. *Phys. Rev.* **1934**, *46*, 618. (b) Dancoff, S. R. *Phys. Rev.* **1950**, *78*, 382. (c) Pople, J. A. *Trans. Faraday Soc.* **1953**, *49*, 1375. (d) Bartlett, R. J. *Annu. Rev. Phys. Chem.* **1981**, *32*, 359. (e) Cremer, D.; He, Z. *J. Phys. Chem.* **1996**, *100*, 6173. (f) Head-Gordon, M.; Lee, T. J. In *Recent Advances in Computational Chemistry*; Bartlett, R. J., Ed.; World Scienctific: Singapore, 1997; Vol. 3, p 221.

(2) (a) Olsen, J.; Christiansen, O.; Koch, H.; Jørgensen, P. *J. Chem. Phys.* **1996**, *105*, 5082. (b) Peterson, K. A.; Dunning, T. H., Jr. *J. Mol. Struct.* **1997**, *400*, 93. (c) Dunning, T. H., Jr.; Peterson, K. A. *J. Chem. Phys.* **1998**, *108*, 4761.

(3) Leininger, M. L.; Allen, W. D.; Schaefer, H. F., III; Sherrill, D. C. *J. Chem. Phys.* **2000**, *112*, 9213.

(4) (a) *Low-Lying Potential Energy Surfaces*, ACS Symposium Series, Vol. 828; Hoffmann, M. R., Dyall, K. G., Eds.; American Chemical Society: Washington, DC, 2002; (b) Fan, P. D.; Piecuch, P. *Adv. Quantum Chem.* **2006**, *51*, 1. (c) Piecuch, P.; Pimienta, I. S. O.; Fan, P.-D.; Kowalski, K. In

Electron Correlation Methodology, ACS Symposium Series, Vol. 958; Wilson, A. K., Peterson, K. A., American Chemical Society: Washington, DC, 2007; p 37.

(5) (a) Buenker, R. J.; Peyerimhoff, S. D. *Theor. Chim. Acta* **1974**, *35*, 33. (b) Siegbahn, P. E. M. *J. Chem. Phys.* **1980**, *72*, 1674. (c) Buenker, R. J.; Krebs, S. In *Recent Advances in Multi-reference Methods*; Hirao, K., Ed.; World Scientific: Singapore, 1999. (d) Sherrill, C. D.; Schaefer, H. F. In *Advances in Quantum Chemistry*; Löwdin, P.-O., Ed.; Academic Press: New York, 1999; Vol. 34, pp 143−269.

(6) (a) Haque, M. A.; Mukherjee, D. *J. Chem. Phys.* **1984**, *80*, 5058. (b) Jeziorski, B.; Monkhorst, H. J. *Phys. Rev. A* **1981**, *24*, 1668. (c) Piecuch, P.; Paldus, J. *Phys. Rev. A* **1994**, *49*, 3479. (d) Máśik, J.; Hubač, I. *Adv. Quantum Chem.* **1999**, *31*, 75. (e) Hubač, I.; Pittner, J.; Eársky, P. *J. Chem. Phys.* **2000**, *112*, 8779. (f) Pittner, J. *J. Chem. Phys.* **2003**, *118*, 10876. (g) Hanrath, M. *J. Chem. Phys.* **2005**, *123*, 084102. (h) Nicolaides, C. A. *Int. J. Quantum Chem.* **2005**, *102*, 250.

(7) (a) Mahapatra, U. S.; Datta, B.; Bandyopadhyay, B.; Mukherjee, D. *Adv. Quantum Chem.* **1998**, *30*, 163. (b) Mahapatra, U. S.; Datta, B.; Mukherjee, D. *J. Chem. Phys.* **1999**, *110*, 6171. (c) Evangelista, F. A.; Allen, W. D.; Schaefer, H. F., III *J. Chem. Phys.* **2007**, *127*, 024102. (d) Evangelista, F. A.; Simmonett, A. C.; Allen, W. D.; Schaefer, H. F., III; Gauss, J. *J. Chem. Phys.* **2008**, *128*, 124104.

(8) (a) Brandow, B. *Rev. Mod. Phys.* **1967**, *39*, 771. (b) Lindgren, I. *J. Phys. B: At. Mol. Opt. Phys.* **1974**, *7*, 2441.

(9) (a) Hoffmann, M. R. *Chem. Phys. Lett.* **1992**, *195*, 127. (b) Hoffmann, M. R. *Chem. Phys. Lett.* **1993**, *210*, 193. (c) Hoffmann, M. R. *J. Chem. Phys.* **1996**, *100*, 6125. (d) Khait, Y. G.; Hoffmann, M. R. *J. Chem. Phys.* **1998**, *108*, 8317.

(10) Davidson, E. R.; Bender, C. F. *Chem. Phys. Lett.* **1978**, *59*, 369.

(11) (a) Cave, R. J.; Davidson, E. R. *J. Chem. Phys.* **1993**, *88*, 5770. (b) Staroverov, V. N.; Davidson, E. R. *Chem. Phys. Lett.* **1998**, *296*, 435.

(12) Chen, F.; Davidson, E. R.; Iwata, S. *Int. J. Quantum Chem.* **2002**, *86*, 256.

(13) Murphy, R. B.; Messmer, R. P. *J. Chem. Phys.* **1992**, *97*, 4170.

(14) (a) Andersson, K.; Malmqvist, P. Å.; Roos, B. O.; Sadlej, A. J.; Wolinski, K. *J. Chem. Phys.* **1990**, *94*, 5483. (b) Andersson, K.; Roos, B. O.; Malmqvist, P. Å.; Widmark, P.-O. *Chem. Phys. Lett.* **1994**, *230*, 391.

(15) Werner, H. J. *Mol. Phys.* **1996**, *89*, 645.

(16) Dyall, K. G. *J. Chem. Phys.* **1995**, *102*, 4909.

(17) (a) Hirao, K. *Chem. Phys. Lett.* **1992**, *190*, 374. (b) Hirao, K. *Int. J. Quantum Chem.* **1992**, *S26*, 517. (c) Choe, Y.-K.; Nakano, Y.; Hirao, K. *J. Chem. Phys.* **2001**, *115*, 621. (d) Nakano, H.; Yamanishi, M.; Hirao, K. *Trends Chem. Phys.* **1997**, *6*, 167. (e) Hirao, K.; Nakayama, K.; Nakajima, T.; Nakano, H. In *Computational Chemistry*; Lesczinski, J., Ed.; World-Scientific: Singapore, 1999; p 227.

(18) Rosta, E.; Surján, P. R. *J. Chem. Phys.* **2002**, *116*, 878.

(19) Angeli, C.; Cimiraglia, R.; Evangelisti, S.; Leininger, T.; Malrieu, J. P. *J. Chem. Phys.* **2001**, *114*, 10252.

(20) (a) Sheppard, M. G.; Freed, K. F. *J. Chem. Phys.* **1981**, *75*, 4525. (b) Freed, K. F. *Acc. Chem. Res.* **1983**, *16*, 137. (c) Sun, H.; Freed, K. F. *J. Chem. Phys.* **1988**, *88*, 2659. (d) Finley, J. P.; Freed, K. F.; Ardent, M. F.; Graham, R. L. *J. Chem. Phys.* **1995**, *102*, 1306. (e) Finley, J. P.; Chaudhuri, R. K.; Freed, K. F. *Phys. Rev. A* **1996**, *54*, 343.

(21) (a) Nakano, H. *J. Chem. Phys.* **1993**, *99*, 7983. (b) Nakano, H.; Nakatani, J.; Hirao, K. *J. Chem. Phys.* **2001**, *114*, 1133.

(22) Kozlowski, P. M.; Davidson, E. R. *J. Chem. Phys.* **1994**, *100*, 3672.

(23) Zaitevskii, A.; Malrieu, J. P. *Theor. Chim. Acta* **1997**, *96*, 269.

(24) (a) Angeli, C.; Cimiraglia, R.; Malrieu, J. P. *J. Chem. Phys.* **2002**, *117*, 9138. (b) Angeli, C.; Borini, S.; Cestari, M.; Cimiraglia, R. *J. Chem. Phys.* **2004**, *121*, 4043. (c) Angelia, C.; Calzado, C. J.; Cimiraglia, J. R.; Malrieu, J. P. *J. Chem. Phys.* **2006**, *124*, 234109.

(25) Finley, J. *J. Chem. Phys.* **1998**, *109*, 7725.

(26) (a) Mahapatra, U. S.; Datta, B.; Mukherjee, D. *J. Phys. Chem. A* **1999**, *103*, 1822. (b) Ghosh, P.; Chattopadhyay, S.; Jana, D.; Mukherjee, D. *Int. J. Mol. Sci.* **2002**, *3*, 733.

(27) Pahari, D.; Chattopadhyay, S.; Das, S.; Mukherjee, D.; Mahapatra, U. S. In *Theory and Applications of Computational Chemistry: The First 40 Years*; Dytkstra, C. E., Frenking, G., Kim, K. S., Scuseria, G. E., Eds.; Elsevier: Amsterdam, The Netherlands, 2005; p 581.

(28) (a) Schucan, T. H.; Weidenmüller, H. A. *Ann. Phys.* **1972**, *73*, 108. (b) Kirtman, B. *J. Chem. Phys.* **1981**, *75*, 798. (c) Malrieu, J. P.; Durand, Ph.; Daudey, J. P. *J. Phys. A* **1985**, *18*, 809. (d) Durand, Ph.; Malrieu, J. P. *Adv. Chem. Phys.* **1987**, *67*, 321, and references therein.

(29) (a) Zaitsevskii, A.; Malrieu, J. P. *Chem. Phys. Lett.* **1995**, *233*, 597. (b) Zaitsevskii, A.; Malrieu, J. P. *Chem. Phys. Lett.* **1996**, *250*, 366.

(30) Witek, H. A.; Choe, Y.-K.; Finley, J. P.; Hirao, K. *J. Comput. Chem.* **2002**, *23*, 957.

(31) (a) Mahapatra, U. S.; Chattopadhyay, S.; Chaudhuri, R. K. *J. Chem. Phys.* **2008**, *129*, 024108. (b) Mahapatra, U. S.; Chattopadhyay, S.; Chaudhuri, R. K. *J. Chem. Phys.* **2009**, *130*, 014101.

(32) (a) Pittner, J.; Čársky, P.; Hubač, I. *Int. J. Quantum Chem.* **2002**, *90*, 1031. (b) Pittner, J.; Demel, O. *J. Chem. Phys.* **2005**, *122*, 181101. (c) Bhaskaran-Nair, K.; Demel, O.; Pittner, J. *J. Chem. Phys.* **2008**, *129*, 184105.

(33) Bauschlicher, C. W.; Langhoff, S. R. *J. Chem. Phys.* **1987**, *86*, 5595.

(34) Andersson, K.; Malmqvist, P. Å.; Roos, B. O. *J. Chem. Phys.* **1992**, *96*, 1218.

(35) Huber, K. P.; Herzberg, G. *Molecular Spectra and Molecular Structure IV. Constants of Diatomic Molecules*; Von Nostrand: New York, 1979.

(36) Van Dam, H. J. J.; Van Lenthe, J. H.; Pulay, P. *Mol. Phys.* **1998**, *93*, 431.

(37) (a) Basis sets were obtained from: Basis Set Exchange, v1.2.2; www.emsl.pnl.gov/forms/basisform.html. (b) Feller, D. The Role of Databases in Support of Computational Chemistry Calculations. *J. Comput. Chem.* **1996**, *17*, 1571–1586. (c) Schuchardt, K. L.; Didier, B. T.; Elsethagen, T.; Sun, L.; Gurumoorthi, V.; Chase, J.; Li, J.; Windus, T. L. Basis Set Exchange: A Community Database for Computational Sciences. *J. Chem. Inf. Model.* **2007**, *47*, 1045–1052.

JP810910N